



Self-Assembly of 2D Lanthanide-Metal Coordination Polymers Based on 5-Nitroisophthalic Acid Linker: Synthesis, Structures, and Luminescence

S.-L. Wang, L.-Y. Zhang & Q. Huang

To cite this article: S.-L. Wang, L.-Y. Zhang & Q. Huang (2015) Self-Assembly of 2D Lanthanide-Metal Coordination Polymers Based on 5-Nitroisophthalic Acid Linker: Synthesis, Structures, and Luminescence, Molecular Crystals and Liquid Crystals, 609:1, 161-170, DOI: [10.1080/15421406.2014.954307](https://doi.org/10.1080/15421406.2014.954307)

To link to this article: <http://dx.doi.org/10.1080/15421406.2014.954307>



View supplementary material [↗](#)



Published online: 11 Apr 2015.



Submit your article to this journal [↗](#)



Article views: 58



View related articles [↗](#)



View Crossmark data [↗](#)

Self-Assembly of 2D Lanthanide-Metal Coordination Polymers Based on 5-Nitroisophthalic Acid Linker: Synthesis, Structures, and Luminescence

S.-L. WANG,¹ L.-Y. ZHANG,¹ AND Q. HUANG^{1,2,*}

¹College of Chemistry and Chemical Engineering, Guangxi University for Nationalities, Nanning, P.R. China

²Guangxi Key Laboratory of Chemistry and Engineering of Forest Products, Nanning, P.R. China

Three 2D novel lanthanide-based metallic coordination frameworks involving the 5-nitroisophthalic acid ligand were characterized by elemental analysis, infrared spectroscopy, thermogravimetric analysis, and single-crystal X-ray diffraction, namely, [Er(NIPH)₂(H₂O)₂](H₂O)₂ (1), [Eu₄(NIPH)₆(H₂O)₈](H₂O)₅ (2), and [Eu₄(NIPH)₆(H₂O)₆](H₂O)₄ (3), synthesized under hydrothermal conditions, self-assemble through Ln₂[NIPH]₂ building blocks to give a 2D coordination layer structure. The adjacent layers stack to form a 3D supramolecular framework through weak interactions, such as hydrogen bonding, π - π interactions, and lone pair- π interactions. However, in 1 and 2 formed 2D 4-connected (4,4) topological network. In addition, in this work the photoluminescent property of the compound 3 has been studied.

Keywords 5-Nitroisophthalic acid; fluorescence; supramolecular network

Introduction

A great deal of effort has been invested in the design and synthesis of coordination polymers due to their intriguing network topologies and promising applications in fields such as catalysis, ion exchange, gas storage, selective adsorption and separation, optics, and magnetic devices [1–2]. Up to now, numerous 1D, 2D, and 3D coordination polymers have been synthesized by the choice of appropriate metal ions and versatile bridging organic ligands [3–4]. As compared with the fruitful reports of transition metal coordination polymers, the assembly of lanthanide coordination networks has had an upsurge of interest in recent years [5]. For the variable coordination numbers and special chemical characteristics of lanthanide ions, they can be used to construct fascinating network topologies, in particular, some reported lanthanide coordination polymers exhibit interesting magnetism and luminescence properties arising from 4f electrons [6].

Considering that the lanthanide ions have high affinities for hard donor atoms like oxygen of carboxylic groups, benzenepolycarboxylate ligands are often employed to link

*Address correspondence to Qin Huang, College of Chemistry and Chemical Engineering, Guangxi University for Nationalities, Nanning 530006, P.R. China. E-mail: huangqinpeking@163.com

Color versions of one or more of the figures in the article can be found online at www.tandfonline.com/gmcl.

the nodes of the single metal ions or metal-carboxylate clusters in lanthanide organic frameworks [7]. For example, the use of 1,4-benzenedicarboxylate has led to a series of lanthanide metalorganic frameworks with novel optical properties [8]. To construct novel architectures, various functional groups such as amine, sulfonate, nitro, and hydroxyl groups have been attached to benzene-polycarboxylate ligands [9–11]. Recently, we have systematically studied supramolecular lanthanide frameworks based on 5-nitroisophthalic acid (H_2NIPH) [11d]. In this work, we used 5-nitroisophthalic acid (H_2NIPH) as the bridge ligand to construct novel lanthanide coordination 2D networks under hydrothermal conditions. We have succeeded in obtaining three new complexes $[\text{Er}(\text{NIPH})_2(\text{H}_2\text{O})_2](\text{H}_2\text{O})_2$ (**1**), $[\text{Eu}_4(\text{NIPH})_6(\text{H}_2\text{O})_8](\text{H}_2\text{O})_5$ (**2**), and $[\text{Eu}_4(\text{NIPH})_6(\text{H}_2\text{O})_6](\text{H}_2\text{O})_4$ (**3**), which were isolated and structurally characterized. Herein, we report their synthesis, structures, thermal gravimetric, and fluorescence properties.

Experimental

Synthesis of Compounds 1–3

$[\text{Er}(\text{NIPH})_2(\text{H}_2\text{O})_2](\text{H}_2\text{O})_2$ (**1**). The reagents of H_2NIPH (2.1 mg, 0.1 mmol), Er_2O_3 (3.8 mg, 0.1 mmol), one drop of nitric acid and 2 mL water were placed in a thick Pyrex tube. The sealed tube was heated at 145°C for 6 days to yield light yellow block-shaped crystals. The crystals were washed with ethanol, dried, and stored under vacuum (66% yield based on Er). Elemental analysis. $\text{C}_{16}\text{H}_{15}\text{ErN}_2\text{O}_{16}$: calcd. C, 29.18, H, 2.30, N, 4.25%; Found: C, 29.16, H, 2.25, N, 4.33%. IR: 3323, 3112, 1714, 1223, 1385, 1245, 1114, 856, 617, and 426.

$[\text{Eu}_4(\text{NIPH})_6(\text{H}_2\text{O})_8](\text{H}_2\text{O})_5$ (**2**). The reagents of H_2NIPH (4.3 mg, 0.2 mmol), Eu_2O_3 (3.5 g, 0.1 mmol), one drop of nitric acid and 2 mL water were placed in a thick Pyrex tube. The sealed tube was heated at 145°C for 6 days to yield light yellow block-shaped crystals. The crystals were washed with ethanol, dried, and stored under vacuum (64% yield based on Eu). Elemental analysis. $\text{C}_{48}\text{H}_{44}\text{Eu}_4\text{N}_6\text{O}_{49}$: calcd. C, 27.50, H, 2.12, N, 4.01%; Found: C, 27.46, H, 2.10, N, 4.03%. IR: 3406, 3013, 1614, 1246, 1375, 1238, 1129, 886, 642, and 419.

$[\text{Eu}_4(\text{NIPH})_6(\text{H}_2\text{O})_6](\text{H}_2\text{O})_4$ (**3**). The reagents of H_2NIPH (6.0 mg, 0.2 mmol), Eu_2O_3 (3.5 mg, 0.1 mmol), one drop of nitric acid and 2 mL water were placed in a thick Pyrex tube. The sealed tube was heated at 145°C for 6 days to yield light yellow block-shaped crystals. The crystals were washed with ethanol, dried, and stored under vacuum (70% yield based on Eu). Elemental analysis. $\text{C}_{48}\text{H}_{40}\text{Eu}_4\text{N}_6\text{O}_{46}$: calcd. C, 28.20, H, 1.97, N, 4.11%; Found: C, 28.26, H, 1.90, N, 4.13%. IR: 3320, 3014, 1642, 1238, 1346, 1242, 1119, 864, 635, and 416.

Materials and Physical Measurements

All the salts were obtained from commercial sources and used without further purification. Elemental (C, H, and N) analyses were performed on a Perkin-Elmer 2400 element analyzer. Infrared (IR) samples were prepared as KBr pellets, and spectra were obtained in the $400\text{--}4000\text{ cm}^{-1}$ range using a Nicolet Avatar 360 FT-IR spectrophotometer. Fluorescence spectra were recorded with F-2500 FL Spectrophotometer analyzer. Thermogravimetric analysis (TGA) experiments were carried out on a NETZSCH TGA thermogravimetric analyzer with a heating rate of $10^\circ\text{C}/\text{min}$ between 20°C and 1000°C under a dry N_2 atmosphere. Powder XRD investigations were carried out on a Bruker D8-advance X-ray diffractometer with $\text{Cu } K_\alpha$ radiation. Single crystal diffraction was carried out on Bruker

Table 1. Crystallographic data and structure refinement details for compounds **1–3**

Complexes	1	2	3
Empirical formula	C ₁₆ H ₁₅ ErN ₂ O ₁₆	C ₄₈ H ₄₄ Eu ₄ N ₆ O ₄₉	C ₄₈ H ₃₈ Eu ₄ N ₆ O ₄₆
Formula weight	658.56	2096.73	2042.68
Temperature	293(2)	296	293(2)
Crystal system	Triclinic	Triclinic	Monoclinic
Space group	<i>P</i> $\bar{1}$	<i>P</i> $\bar{1}$	<i>P</i> 2 ₁ / <i>c</i>
<i>a</i> (Å)	9.656(6)	11.3075(18)	13.806(4)
<i>b</i> (Å)	10.441(7)	11.9981(19)	22.074(6)
<i>c</i> (Å)	13.569(11)	12.599(2)	23.061(5)
α (°)	112.195(7)	77.049(2)	90
β (°)	91.263(10)	87.796(2)	119.351(13)
γ (°)	115.080(7)	79.654(2)	90
Volume (Å ³)	1119.8(14)	1638.8(5)	6126(3)
<i>Z</i>	2	1	4
<i>D</i> _{calc} mg/m ^{−3}	1.953	2.125	2.215
μ	3.831	3.899	4.165
<i>F</i> ₍₀₀₀₎	642	1018	3952
GOF on <i>F</i> ²	1.026	1.050	1.103
<i>R</i> 1	0.0257	0.0218	0.1101
<i>wR</i> 2	0.0663	0.0592	0.2201
<i>R</i> 1 (all data)	0.0285	0.0242	0.2138
<i>wR</i> 2 (all data)	0.0685	0.0610	0.2723

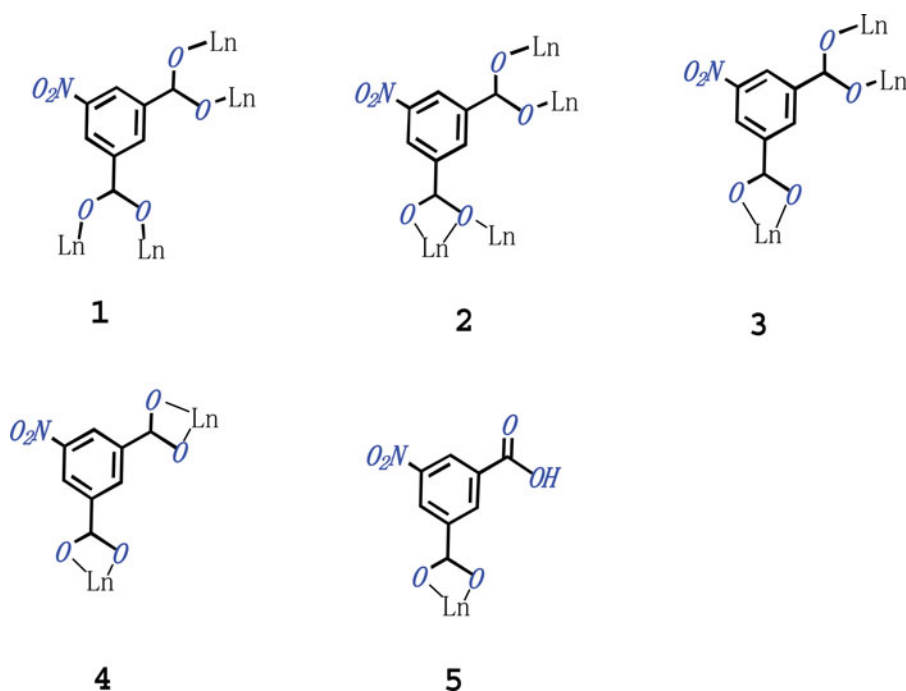
$$^a R_1 = \sum(|F_o| - |F_c|) / \sum |F_o|; wR_2 = [\sum w(|F_o|^2 - |F_c|^2)^2 / \sum w(|F_o|^2)]^{1/2}$$

Apex II Smart X-ray diffractometer. Crystal structure determination: Single crystal X-ray diffraction (XRD) data collections of **1–3** were performed on a Bruker Apex II CCD diffractometer operating at 50 kV and 30 mA using Mo *K* α radiation ($\lambda = 0.71073$). Data collection and reduction were performed using the Apex II software. Multiscan absorption corrections were applied for all the data sets using the APEX II program. All structures were solved by direct methods and refined by full-matrix least squares on *F*² using the SHELXTL program package. All non-hydrogen atoms were refined with anisotropic displacement parameters. Hydrogen atoms attached to carbon were placed in geometrically idealized position and refined using a riding model. Hydrogen atoms on water molecules were located from difference Fourier maps and were refined using riding model. Hydrogen atoms of lattice water molecules of O₄₆ (complex **3**) is not located due to the disorder but were added in the formula. The crystallographic data for **1–3** are shown in Table 1. CCDC numbers: 866332, 872044, and 866333 for all structures are contained in the supplementary crystallographic data for this paper.

Results and Discussion

Description of the Structure

2D layer of [Er(NIPH)₂(H₂O)₂](H₂O)₂ (1). The X-ray single crystal diffraction studies performed on **1** reveals that each asymmetric unit contains one eight-coordinated Er ion, five NIPH ligands, two coordinated water, and two lattice water molecules. As shown in Fig. 1(a), each Er is coordinated by six oxygen atoms from five different NIPH ligands and



Scheme 1. The coordination modes of H_2NIPH ligand in **1–3**.

two oxygen atoms from coordinated water molecules. The Er–O bond distances are in the range of 2.24–2.79 Å. Two Er atoms are joined together by two carboxylate groups to form a dinuclear building block with an Er–Er distance of 4.93 Å. The adjacent dinuclear building blocks connect to each other through NIPH ligands resulting in the formation of 2D layer framework with 4,4 square lattice topology. In addition, there is O–H···O between water molecules and uncoordinated carboxylate groups. Finally, the 3D supramolecular network is stabilized by interlayer π – π stacking interactions.

$[\text{Eu}_4(\text{NIPH})_6(\text{H}_2\text{O})_8](\text{H}_2\text{O})_5$ (**2**). The X-ray single crystal diffraction studies performed on **2** reveals that both Eu1 and Eu2 are eight-coordinated polyhedron made of six oxygen atoms from five NIPH ligands and two oxygen atoms from the lattice water molecules. In **2**, NIPH also adopts three coordination modes: 2-NIPH, 3-NIPH, and 4-NIPH (Scheme 1). Taking the pairs of Ln as nodes respectively, the 2D layer can be simplified to a 4,4 topology [Fig. 2(c)]. And the adjacent layers finally connect to each other via the π – π stacking interactions to generate a 3D framework [Fig. 2(b)]. Due to the numerous lattice water molecules in the structure, there are strong hydrogen-bonding interactions, which further strengthened the 3D framework. It appears that there are abundant of hydrogen-bonding interactions in the framework of **2**, which include the following contacts: (a) between the water molecules and nitro-oxygen, (b) between water molecules and uncoordinated carboxylic-oxygen, and (c) between C–H groups of NIPH and nitro-oxygen atoms. As a result, 3D supramolecular architecture is formed.

$[\text{Eu}_4(\text{NIPH})_6(\text{H}_2\text{O})_6](\text{H}_2\text{O})_4$ (**3**). Each asymmetric unit of **3** consists of four crystallographically independent Eu ions, six distinct NIPH ligands, and six coordinated water and four lattice water molecules. The Eu1 and Eu2 center are nine-coordinated by eight oxygen

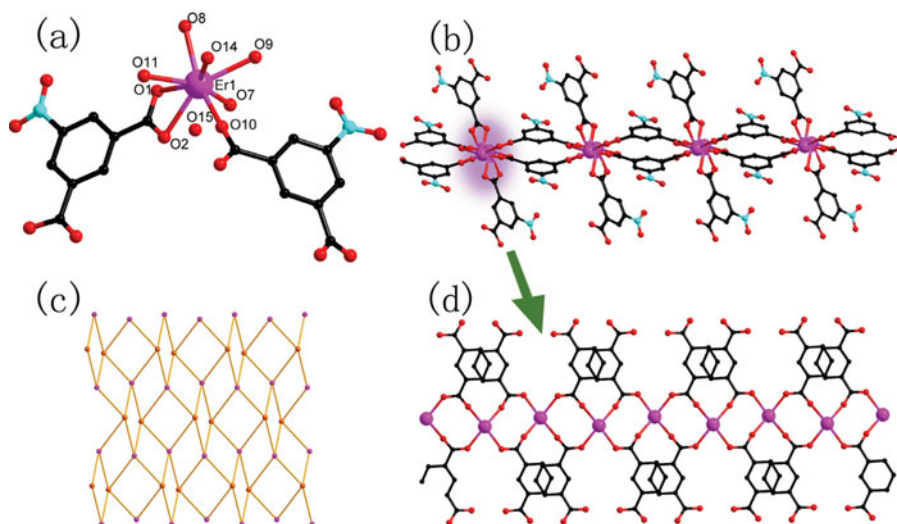


Figure 1. (a) View of the asymmetric unit of structure **1**. (b) Packing diagram of the layer structure. (c) View of the 2D 4-connected (4, 4) topological network in **1**. (d) View of an infinite Er—O—C—O—Er—chain along a axial.

atoms from six NIPH and one coordinated water oxygen atom. The Eu3 is eight-coordinated by four oxygen atoms from four NIPH ligands and four oxygen atoms from coordinated water molecules. But Eu4 is seven-coordinated by seven oxygen atoms from six NIPH ligands. The distances of Eu—O bonds range from 2.35 to 2.94 Å. It is noteworthy that NIPH ligand in **3** adopts four different coordination modes: 1-NIPH, 2-NIPH, 3-NIPH, and 4-NIPH (Scheme 1). As far as we know, it is rare that one ligand coordinated to the metal with four or more coordination modes in the identical compound. As shown in Figs. 3(c) and (d), each NIPH ligand contributes two carboxylate groups to link two adjacent Eu(III) ions to form an infinite —Eu—O—C—O—Eu— zigzag chain along a axial. Then adjacent 1D zigzag chains are further bridged by another NIPH ligand along *c* axial to form 2D wavelike layers [Fig. 3(b)]. Furthermore, the adjacent layers finally connect to each other via strong lone pair- π interactions to generate a 3D framework. Strong hydrogen bonding interactions play important roles in the strengthening of the 3D framework.

Spectroscopic Properties and Powder X-Ray Diffraction

In the FTIR spectra of compounds **1–3**, the absorption bands in the region 3300–3350 cm^{-1} indicate the presence of free and/or coordinated water molecules. The bands in the region 3100–3060 cm^{-1} can be ascribed to C—H stretching vibrations of the benzene ring. The band at around 1700 cm^{-1} for **1** demonstrates the existence of COOH, whereas the absence of a band at around 1700 cm^{-1} for **2–3** indicates the deprotonation of COOH to form COO^- anions.

Simulated and experimental powder X-ray diffraction (PXRD) patterns of **1–3** are shown in Fig. S1. All the peaks in the recorded curves approximately match those in the simulated curves generated from single-crystal diffraction data, which confirms the phase purity of the as-prepared products.

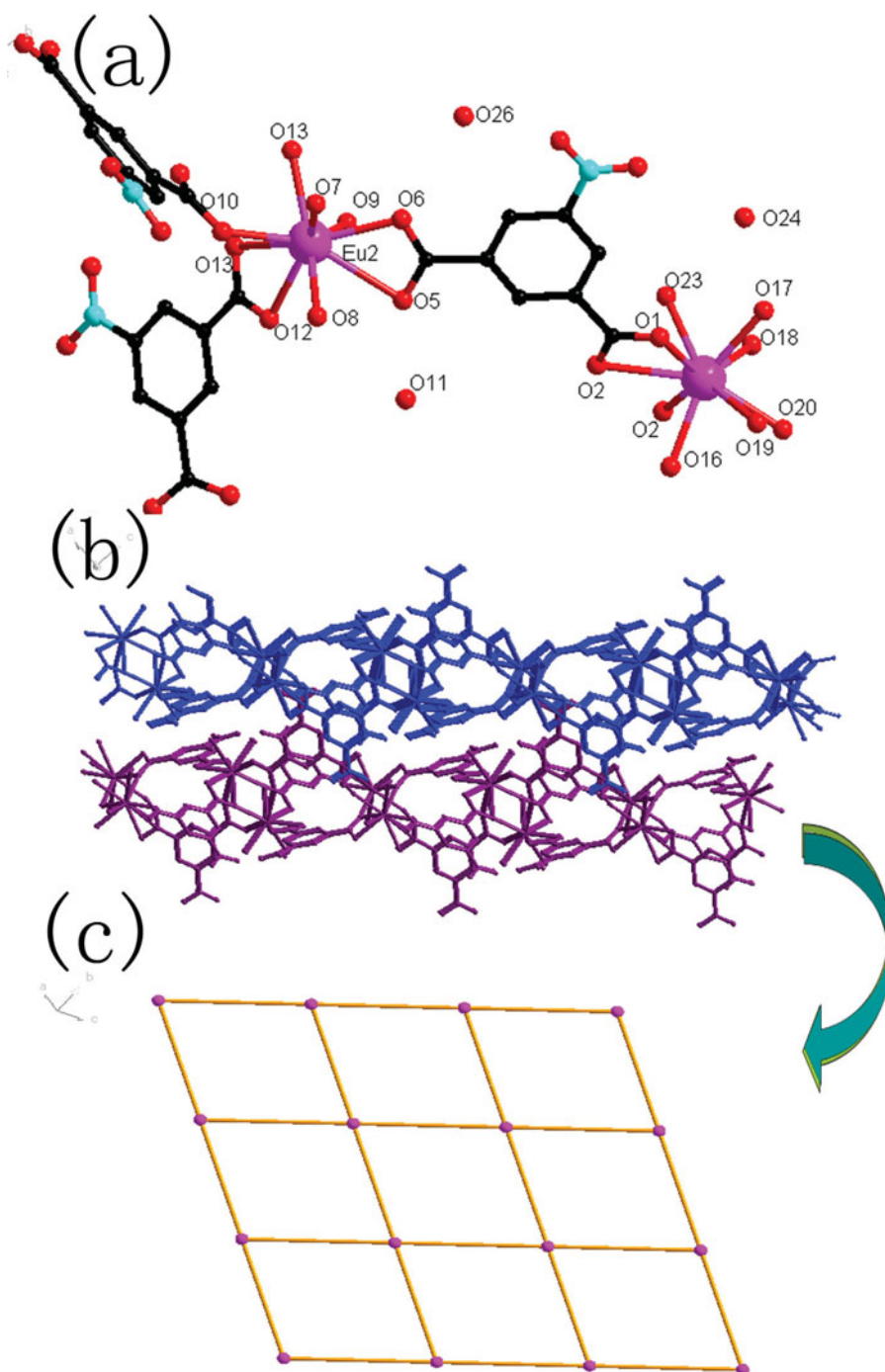


Figure 2. (a) View of the asymmetric unit of structure **2**. (b) ABAB layer structure of **2**. (c) View of the 2D 4-connected (4, 4) topological network in **2**.

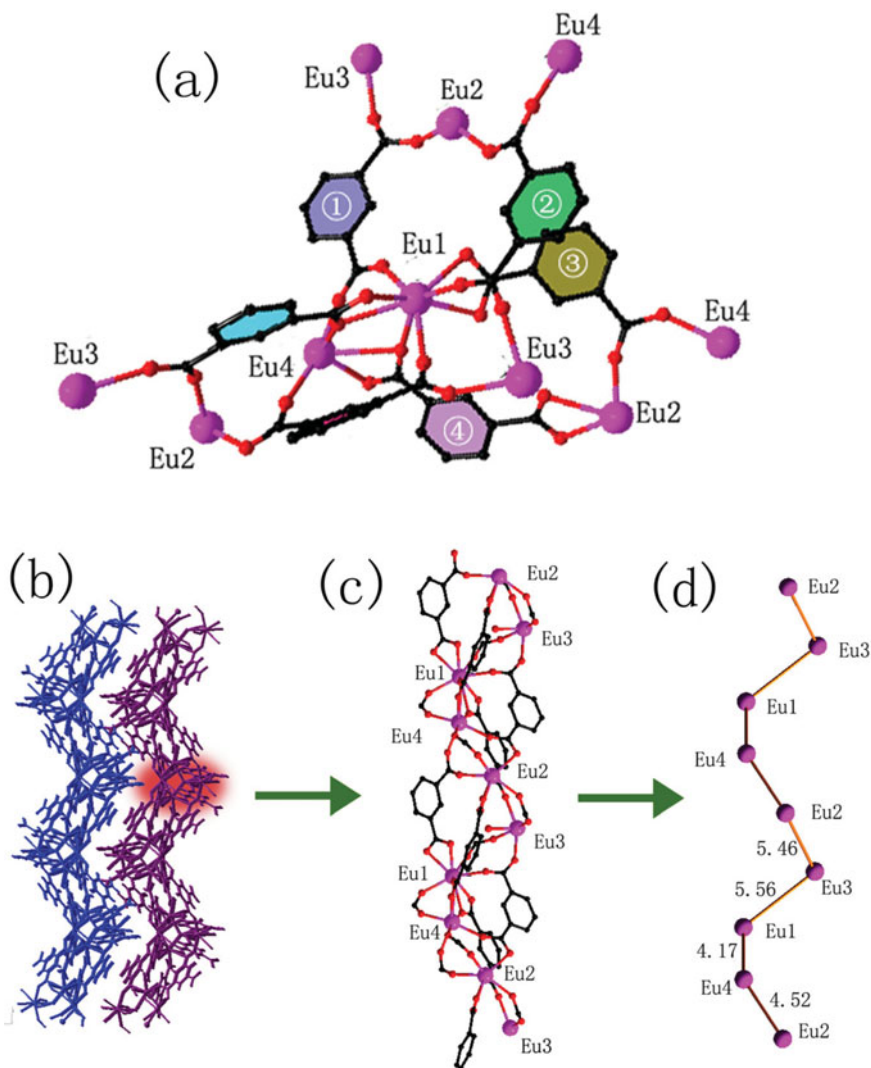


Figure 3. (a) View of the asymmetric unit of structure **3**, showing the six different coordination model of H_2NIPH ligand. (b) 2D-layer structure of **3**. (c) View of an infinite $-\text{Eu}-\text{O}-\text{C}-\text{O}-\text{Eu}-$ chain along a axial. (d) Perspective view of the $-\text{Eu}-\text{O}-\text{C}-\text{O}-\text{Eu}-$ chain along a axial.

Thermal Properties and Luminescence Properties

To study the thermal behavior of the compounds, TGA of **1–3** were carried out from 20°C to 1000°C at the heating rate of 10°C/min in N_2 atmosphere. The TGA curves show that there are two or three main events of weight loss as shown in Fig. 4. For complex **1**, the TGA indicates that **1** lose of 6.9% of total weight in the 50°C–200°C temperature range, corresponding to the removal of the four water molecules (calcd. 6.5%). When the temperature holds on rising, the products lose 37.2% of the total weight in the 250°C–600°C temperature range, corresponding to the removal of two NIPH ligands (calcd. 36.9%). **2** losses 12.9% of the total weight in the 50°C–250°C temperature range, corresponding to

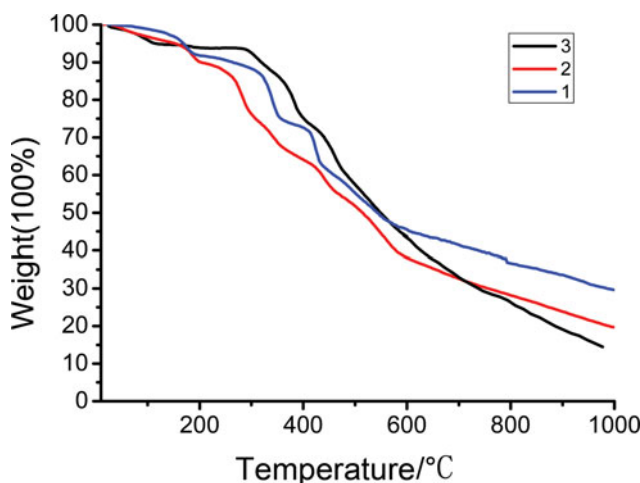


Figure 4. TGA curves of complexes **1–3**.

the removal of thirteen water molecules, when the temperature holds on rising, the products lose 59% of the total weight in the 250°C–650°C temperature range, corresponding to the removal of the H₂NIPH ligands. Complex **3** loses 8.5% of the total weight in 50°C–250°C temperature range, which corresponding to the removal of 10 water molecules, and then loses 70% at the 250°C–700°C temperature range, corresponding to the removal of the H₂NIPH ligands.

The luminescent spectra of these compounds were recorded in the solid state at room temperature. Taking into account the excellent luminescent properties of Eu(III) ion, the luminescence of **3** as shown in Fig. 5. The emission spectrum of **3** consists of four bands of

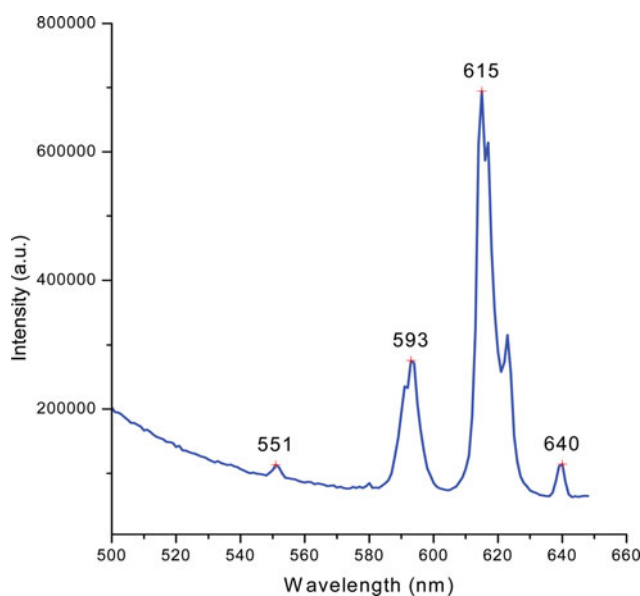


Figure 5. The luminescence curves of **3**.

551, 593, 615, and 640 nm. These two main peaks typically correspond to the characteristic transition of $^5D_0-^7F_J$ ($J = 0-4$) of Eu(III) ions via a ligand-to-metal energy mechanism. The most intense emission at 615 nm is attributed to $^5D_0-^7F_2$ transition induced by the electric dipole, suggesting that the interactions between the complex and its local environment are strong [12] and that the ligand is favorable for the sensitization of red luminescence for Eu(III) ions under the experimental conditions used [13]. The medium strong emission at 593 nm and 640 nm are corresponding to the magnetic dipole induced $^5D_0-^7F_1$ transition and the electric dipole induced $^5D_0-^7F_4$ transition, respectively. The presence of the $^5D_0-^7F_0$ transition at 551 nm indicates that the Eu(III) in **3** occupies sites with low symmetry and possess a noncentrosymmetric coordination environment [14]. As is well known, the intense ratio of $^5D_0-^7F_2/^5D_0-^7F_1$ was widely used as a measurement of the symmetry of the rare earth. The intense ratio of $^5D_0-^7F_2/^5D_0-^7F_1$ is about 2.7, much higher than 0.67, a typical value for a centrosymmetric Eu^{3+} center, which testifies the low site symmetry of Eu(III) in as well. Moreover, the emission spectrum of **615** exhibits plenty of small splittings, which is useful for confirming the local site symmetry of the lanthanide ions [15].

Conclusions

We have obtained three lanthanide-metal coordination polymers based on the 5-nitroisophthalic acid linker. The compounds **1–3** are constructed by two or more types of coordination modes of H_2NIPH and form 2D frameworks, in these complexes the 3D supramolecular structure forms through hydrogen bonding and $\pi-\pi$ interactions. The 2D 4-connected (4, 4) topological network topologies structures formed in **1** and **2**. These compounds show strong photoluminescence at room temperature, respectively, and may be good candidates for potential luminescence materials.

Funding

This work was supported by the NSF of Guangxi Province (No. 2012GXNSFAA053031), Guangxi Department of Education (201203YB071), the Innovation Project of Guangxi University for Nationalities (No. gxun-chx2013096), and the open fund of Key Laboratory of Guangxi Key Laboratory of Chemistry and Engineering of Forest Products (No. GXFC 13–08).

References

- [1] (a) Moulton, B., & Zaworotko, M. J. (2001). *Chem. Rev.*, *101*, 1629–1658. (b) Uemura, K., Kitagawa, S., Fukui, K., & Saito, K. A. (2004). *J. Am. Chem. Soc.*, *126*, 3817–3828. (c) Rao, C., Natarajan, S., & Vaidhyanathan, R. (2004). *Angew. Chem., Int. Ed.*, *43*, 1466–1496. (d) Yaghi, O. M., Li, H., Davis, C., Richardson, D., Groy, T., & Acc, L. (1998). *Chem. Res.*, *31*, 474–484. (e) Eddaoudi, M., Kim, J., Rosi, N., Vodak, D., Wachter, T. et al. (2002). *Science*, *295*, 469–472.
- [2] (a) Chui, S. S., Lo, Y., Charmant, S. M. F., Orpen, J. P. H., & Williams, G. (1999). *Science*, *283*, 1148–1150. (b) Barthelet, K., Marrot, J., Riou, D., & Ferey, G. (2002). *Angew. Chem., Int. Ed.*, *41*, 281–284. (c) Kitagawa, S., Kitaura, R., & Noro, S. I. (2004). *Angew. Chem., Int. Ed.*, *43*, 2334–2375.
- [3] (a) Hagrman, P. J., Hagrman, D., & Zubieta, J. (1999). *Angew. Chem., Int. Ed.*, *38*, 2638–2684. (b) Uemura, K., Kitagawa, S., Kondo, M., Fukui, K., Kitaura, R., Chang, H. C., & Mizutani, T. (2002). *Chem. Eur. J.*, *8*, 3586–3600. (c) Zhang, Z. H., Shen, Z. L., Okamura, T., Zhu, H. F., Sun, W. Y., et al. (2005). *Cryst. Growth. Des.*, *5*, 1191–1197. (d) Li, J. R., Bu, X. H., & Zhang,

- R. H. (2004). *Inorg. Chem.*, *43*, 237–244. (e) Sun, Y. Q., Zhang, J., Chen, Y. M., & Yang, G. Y. (2005). *Angew. Chem., Int. Ed.*, *44*, 5814–5817.
- [4] (a) Wan, Y. H., Zhang, L. P., Jin, L. P., Gao, S., Lu, S. Z. (2003). *Inorg. Chem.*, *42*, 4985–4994. (b) Chu, D. Q., Xu, J. Q., Duan, L. M., Wang, T. G., Tang, A. Q., & Ye, L. (2001). *Eur. J. Inorg. Chem.*, 1135–1137. (c) Shi, Q., Cao, R., Sun, D. F., Hong, M. C., & Liang, Y. C. (2001). *Polyhedron*, *20*, 3287–3293.
- [5] (a) Zhou, Y. F., Hong, M. C., & Wu, X. T. (2006). *Chem. Commun.*, 135–143. (b) Cheng, J. W., Zhang, J., Zheng, S. T., Zhang, M. B., Yang, G. Y. (2006). *Angew. Chem., Int. Ed.*, *45*, 73–77. (c) Figuerola, A., Diaz, C., Ribas, J., Tangoulis, V., Granell, J., et al. (2003). *Inorg. Chem.*, *42*, 641–649. (d) Pan, L., Adams, K. M., Hernandez, H. E., Wang, X. T., Zheng, C., et al. (2003). *J. Am. Chem. Soc.*, *125*, 3062–3067. (e) Gheorghe, R., Cucos, P., Andruh, M., Costes, J. P., Donnadieu, B., et al. (2006). *Chem. Eur. J.*, *12*, 187–203. (f) Eddaoudi, M., Moler, D. B., Li, H., Chen, B., Reineke, T. M., et al. (2001). *Acc. Chem. Res.*, *34*, 319–330. (g) De Lill, D. T., Gunning, N. S., & Cahill, C. L. (2005). *Inorg. Chem.*, *44*, 258–266.
- [6] (a) Daiguebonne, C., Kerbellec, N., Bernot, K., Gerault, Y., Deluzet, A., Guillou, O. (2006). *Inorg. Chem.*, *45*, 5399–5406. (b) Zhao, B., Chen, X. Y., Cheng, P., Liao, D. Z., Yan, S. P., & Jiang, Z. H. (2004). *J. Am. Chem. Soc.*, *126*, 15394–15395. (c) Osa, S., Kido, T., Matsumoto, N., Re, N., Pochaba, A., & Mrozinski, J. (2004). *J. Am. Chem. Soc.*, *126*, 420–421. (d) Mishra, A., Wernsdorfer, W., Abboud, K. A., & Christou, G. (2004). *J. Am. Chem. Soc.*, *126*, 15648–15649.
- [7] (a) Zheng, X. J., Wang, Z. M., Gao, S., Liao, F. H., Yan, C. H. et al. (2004). *Eur. J. Inorg. Chem.*, *43*, 2968–2973. (b) Rosi, N. L., Kim, J., Eddaoudi, M., Chen, B. L., O’Keeffe, M. et al. (2005). *J. Am. Chem. Soc.*, *127*, 1504–1518.
- [8] (a) Reineke, T. M., Eddaoudi, M., O’Keeffe, M., & Yaghi, O. M. (1999). *Angew. Chem., Int. Ed.*, *38*, 2590–2594. (b) Reineke, T. M., Eddaoudi, M., Fehr, M., Kelley, D., & Yaghi, O. M. (1999). *J. Am. Chem. Soc.*, *121*, 1651–1657. (c) Pan, L., Zheng, N., Wu, Y. G., Han, S., Yang, R. Y., et al. (2001). *Inorg. Chem.*, *40*, 828–830.
- [9] (a) Sun, D. F., Cao, R., Sun, Y. Q., Bi, W. H., Yuan, D. Q., et al. (2003). *Chem. Commun.*, 1528–1529. (b) Tao, J., Yin, X., Jiang, Y. B., Huang, R. B., & Zheng, L. S. (2003). *Inorg. Chem. Commun.*, *6*, 1171–1174. (c) Sun, Z. M., Mao, J. G., Sun, Y. Q., Zeng, H. Y., & Clearfield, A. (2004). *Inorg. Chem.*, *43*, 336–341.
- [10] (a) Tao, J., Yin, X., Wei, Z. B., Huang, R. B., & Zheng, L. S. (2004). *Eur. J. Inorg. Chem.*, 125–133. (b) Wang, Z., Nfor, H. Q., & You, E. N. (2005). *Cryst. Eng. Comm.*, *7*, 578–585. (c) Ye, J., Zhang, W., Ye, P., Yin, K. Q., Ye, W. R., et al. (2006). *Inorg. Chem. Commun.*, *9*, 744–747.
- [11] (a) Luo, J. H., Hong, M. C., Wang, R. H., Cao, R., Han, L., et al. (2003). *Inorg. Chem.*, *42*, 4486–4488. (b) Luo, J. H., Hong, M. C., Wang, R. H., Cao, R., Han, L., et al. (2003). *Eur. J. Inorg. Chem.*, 2705–2710. (c) Abourahma, H., Moulton, B., Kravtsov, V., & Zaworotko, M. J. (2002). *J. Am. Chem. Soc.*, *124*, 9990–9991. (d) Ye, J. W., Wang, J., Zhang, J. Y., Zhang, P., & Wang, Y. (2007). *Cryst. Eng. Comm.*, *9*, 515–523. (e) Ren, Y. X., Chen, S. P., Gao, S. L., & Shi, Q. Z. (2006). *Inorg. Chem. Commun.*, *9*, 649–653.
- [12] Xu, Q., Li, L., Liu, X., & Xu, R. (2002). *Chem. Mater.*, *14*, 549–555.
- [13] Gu, X. & Xue, D. (2007). *Cryst. Eng. Comm.*, *9*, 471–477.
- [14] Zhao, B., Chen, X.-Y., Cheng, P., Liao, D. Z., & Yan, S. P. et al. (2004). *J. Am. Chem. Soc.*, *126*, 15394–15395.
- [15] Forsberg, J. H. (1973). *Coord. Chem. Rev.*, *10*, 195–226.